

# Effect of Process Parameters on Residual Stress Distribution in Poly(Ethylene Terephthalate) Fibers and Films as Revealed by Chemical Etching

V. B. GUPTA,\* J. RADHAKRISHNAN,<sup>†</sup> and S. K. SETT<sup>‡</sup>

Textile Technology Department, Indian Institute of Technology, New Delhi 110 016, India

## SYNOPSIS

Poly(ethylene terephthalate) fibers and films produced by varying process parameters, such as production speed and medium, temperature and rate of drawing, were annealed at temperatures between 100 and 250°C in the free-to-shrink and constant-length conditions. The as-spun, as-drawn, and drawn and annealed samples were etched in 40% aqueous methylamine at room temperature for 4 h. The etch patterns were examined on a scanning electron microscope and were found to be related mainly to residual stress and its distribution in the samples and thereby to sample morphology. The studies clearly bring about the important role played by the processing history. © 1995 John Wiley & Sons, Inc.

## INTRODUCTION

Poly(ethylene terephthalate) (PET) fibers and films with different mechanical and thermal histories are known to exhibit different stress cracking patterns when exposed to 40% aqueous methylamine.<sup>1-9</sup> The stress cracking has been shown to occur only when a specimen supports an internal or externally applied stress, above a critical level. Sweet and Bell have shown<sup>1</sup> that the crack density in a filament increases as the draw ratio is increased. The increased cracking is associated with an increase in the magnitude of the internal residual stress resulting from enhancement of molecular orientation during drawing. Because of this, crack density and fiber birefringence were found to correlate well. On subjecting the fiber to shrinkage or annealing at low temperatures for a short time, internal residual stress can relax and a decrease in crack density occurs. At higher temperatures or at longer times, fur-

ther crystallization occurs, and this results in a new residual stress field, and crack density can again increase.

Murray et al.<sup>3</sup> interpreted their results on amine etching of PET fiber in terms of Prevorsek's model.<sup>10</sup> Chauhan et al.<sup>4</sup> also explained the appearance of longitudinal and transverse cracks in amine-etched PET fibers on the basis of the existence of two types of amorphous domains, which had been proposed by Prevorsek.<sup>10</sup> A degradative etching technique for PET using *n*-propylamine was employed by Baker<sup>5</sup> to disclose several different degrees of structural order in uniaxially and biaxially stretched films. He hypothesized that these structures were developed in the films during fabrication processes and represented the strain distribution caused by the fabricating stresses. Chu and Wilkes<sup>6</sup> investigated the bulk morphology of PET films and fibers following chemical etching with *n*-propylamine, using scanning electron microscopy. A surface network structure was observed in the etched samples, and the nature of this network depended on the mechanical and thermal history of the sample. Adams<sup>7</sup> also found similar structures using *n*-propylamine etchant on drawn PET films.

In the present investigation, micrographs of the cracking patterns, after chemical etching with 40% methylamine, of PET fibers and films with different

\* To whom correspondence should be addressed.

<sup>†</sup> Present address: Department of Organic and Polymeric Materials, Tokyo Institute of Technology, O-okayama, Tokyo 152, Japan.

<sup>‡</sup> Present address: College of Textile Technology, Serampore-712 201, India.

processing histories were obtained with the help of scanning electron microscopy. The correlation of cracking pattern with the residual stress and residual stress distribution, which in turn are dependent on the processing history, and their relation with sample morphology have been critically examined.

## EXPERIMENTAL

### Starting Samples

#### Fibers

*Monofilament.* Single filaments of 130 denier were spun from fiber-grade PET chips in a laboratory spinning unit at a spinning temperature of 285°C. The filaments were quenched in water at around 5°C, 25 cm below the spinneret, before being wound at 10 m/min.

*Low Oriented Yarn (LOY).* Multifilament PET yarns 165/36/0, i.e., of 165 denier, 36 filaments, and 0 twist, which had been produced on an industrial unit at a wind-up speed of 1000 m/min by M/s Orkay Polyester, Bombay, India, were also used.

#### Film

A 80- $\mu\text{m}$  thick, 30-mm wide film was melt cast from fiber-grade PET chips and quenched on chilled rollers before being wound at 10 m/min on an industrial unit by M/s Garware Polyesters, Aurangabad, India.

### Uniaxial Drawing of Samples

#### Drawing of LOY in Air at 90°C

The LOY produced at 1000 m/min was uniaxially stretched on a laboratory drawing machine by passing it over a heater plate of length 25 cm kept at a temperature of 90°C to a draw ratio of 4.2 at a strain rate of 20  $\text{min}^{-1}$ .

#### Drawing of Film and Filaments in Water at 70°C

PET film and monofilament produced at 10 m/min were drawn to draw ratios of about 4.2 in water at 70°C in two stages in a water bath of length 70 cm at strain rates between 2 to 3  $\text{min}^{-1}$ .

#### Measurement of Drawing Stress

The tension in the running filament or film as it emerged from the heater plate or water bath and before it was taken up by the draw rollers was measured with the help of a Rothschild R 1192 electronic tensiometer.

### Heat Setting

The samples were heat-set for 3 min under two conditions, viz. while free to relax (to be designated as free-annealed, or FA) and at constant length (to be designated as taut-annealed, or TA) in a silicone oil bath isothermally at temperatures between 100 and 250°C. The heat-set samples, after removal from the bath, were first allowed to come to room temperature and then thoroughly washed with carbon tetrachloride after which they were dried. The dried samples were stored in a temperature- and humidity-controlled laboratory.

### Birefringence

A polarizing microscope fitted with a tilting compensator was used to measure the sample birefringence. The thickness of the film was measured with the help of a precision digital micrometer, while the diameter of the fiber was measured with the help of an eyepiece micrometer.

### Density

The density of the samples was estimated with the help of density gradient column.

### Chemical Etching

All degradation experiments were carried out at 25°C using approximately 20 mg of sample in 20 mL of 40% aqueous methylamine. The experiment was carried out with the fiber sample in an unconstrained condition inside a stoppered bottle to avoid loss of gaseous methylamine from the solution, which was agitated. After treatment for 4 h, the samples were washed thoroughly with distilled water and then dried and stored in a conditioned laboratory.

### Scanning Electron Microscopy

The amine-etched PET samples were gold coated prior to being studied in a Cambridge S 360 stereoscan scanning electron microscope in the secondary electron mode. All the micrographs have been reproduced at magnifications of around 500–800.

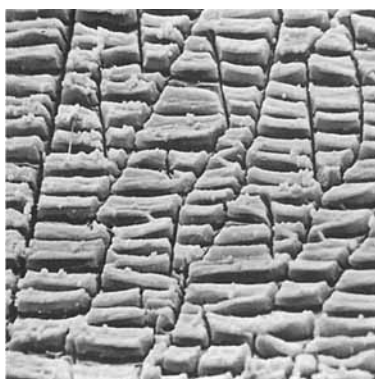
## RESULTS AND DISCUSSION

### As-cast film and As-spun Fiber

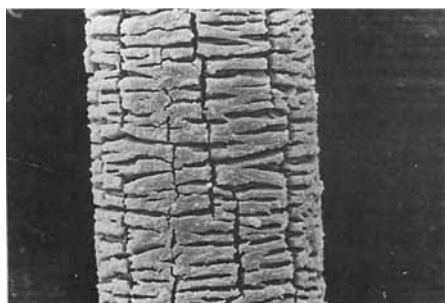
The methylamine etching of undrawn film and fiber samples did not show any cracking patterns, and

**Table 1** Drawing Conditions and Some Physical Characteristics of Drawn Film and Fiber Samples

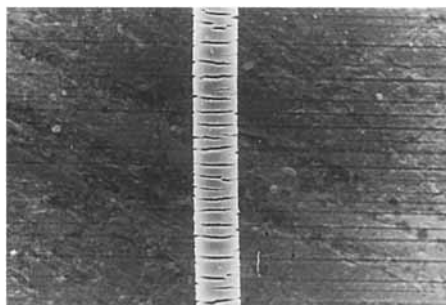
Sample	Drawing Conditions					Birefringence	Density (g/cm <sup>3</sup> )	Diameter/Thickness ( $\mu\text{m}$ )
	Draw Ratio	Temp. ( $^{\circ}\text{C}$ )	Medium	Strain Rate (min <sup>-1</sup> )	Drawing Stress (MPa)			
LOY-based	4.1	90	Air	20	129	0.216	1.362	12
Film	4.16	70	Water	2	37	0.184	1.360	45
Monofilament	4.16	70	Water	2.5	39	0.188	1.360	80



(A)



(B)



(C)

**Figure 1** Crack patterns in amine-etched, as-drawn PET samples: (a) water-drawn film ( $\times 515$ ), (b) water-drawn monofilament ( $\times 560$ ), and (c) air-drawn low oriented yarn ( $\times 560$ ).

hence the micrographs are not reproduced here. The samples degraded homogeneously with a uniform reduction in their dimensions.

### As-drawn Samples

Some physical characteristics of the as-drawn samples along with their processing conditions are summarized in Table I. All the samples are well-oriented and their density values suggest a crystallinity of around 26%. The stress cracking pattern of methylene-etched water-drawn film, water-drawn monofilament, and air-drawn LOY-based fibers are shown in Figures 1 (a), (b), and (c). The etched film and monofilament samples show some irregular longitudinal cracks. Between the longitudinal cracks, stacks of interconnected rectangular blocks, which result from the formation of transverse cracks, can be seen. The interconnected blocks form a network structure, the distance between the transverse cracks being 2–5  $\mu\text{m}$ . The distance between the longitudinal cracks, on the other hand, is 8–20  $\mu\text{m}$ . It is noteworthy that while the longitudinal cracks are very irregular, the transverse cracks show some regularity.

In contrast to the complex crack patterns of the as-drawn film and monofilament, the LOY-based drawn fiber shows a relatively simpler crack pattern. Here the cracks are predominantly transverse to the fiber axis along the cylindrical filament with a low helix angle and a small pitch in the axial direction causing most of the cracks to form a spiral path along the fiber. No longitudinal cracks can be detected. To explain these results, the physical basis for the origin of such cracks in terms of sample morphology will be briefly discussed.

According to the reported literature,<sup>1-9</sup> the cracks appear due to the presence of internal stresses arising mainly from the drawing process. The stresses will principally reside in the amorphous regions and at the boundaries of the crystals. The cracks appearing in the etched PET samples would thus be expected to be a fingerprint of the overall morphol-

ogy of the sample. The structural models for as-drawn PET fibers envisage the presence of irregularly arranged entities in which the crystalline and amorphous phases are not distinctly separated.<sup>11</sup> The model of Prevorsek<sup>10</sup> envisages a PET fiber to be made up of three phases, viz. a crystalline phase, an amorphous intrafibrillar phase, and an interfibrillar amorphous phase; though in the as-drawn state, the entities may not be arranged in as regular a geometry as described by the model of Prevorsek. Oudet and Bunsell<sup>12</sup> proposed a macrofibrillar structure that is superimposed on the microfibrillar structure of Prevorsek. In their model the macrofibrils take the form of cylinders with diameters of between 200 and 500 nm while the microfibrils have estimated diameters of 15–20 nm. During chemical etching, the highly stressed intermicro- or macrofibrillar regions will be the first to be removed, giving rise to longitudinal cracks while the etching of the intrafibrillar or intercrystalline regions will give rise to transverse cracks. It must be emphasized, however, that the spacing of the longitudinal and transverse cracks may not correlate with the morphological model because the residual stress field is not uniform.

The nonuniformity of the residual stress distribution in the water-drawn film and monofilament can be attributed to the following reason. Both monofilament and film are produced by quenching in water. The temperature gradient will be more pronounced in thick monofilaments. As a result there will be a greater degree of radial nonuniformity in thick filaments giving rise to a more prominent skin-core effect, the skin having a relatively higher orientation than the core. This radial differentiation is carried over to the drawn fiber also. The residual stress distribution will consequently be very nonuniform in the drawn monofilaments.

In the case of film sample also, there will be variation in molecular orientation across the thickness due to the above reason. These variable conditions in the residual stress distribution explain the rather wide range of distances between the cracks. Sweet and Bell<sup>1</sup> also observed the average distance between cracks to be approximately 4–8  $\mu\text{m}$ , which appear to leave large areas of the sample unaffected.<sup>2</sup> They stated that since crystalline regions are only 100 Å or less in size, one might expect that these cracks, which are a few microns apart, would only distort a small percentage of the crystals within the sample. However, according to these authors,<sup>1,2</sup> one must not rule out the existence of submicroscopic cracks that did not develop into macroscopic size. These could be responsible for crystalline distortion and rupture at the microlevel.

The observed differences in the crack pattern of the LOY-based drawn fiber in contrast to those of the film and monofilament would be expected to relate to the differences in processing conditions. The data on the strain rates used and the drawing stresses that were generated are given in Table I. The drawing stress is the highest for the LOY-based yarn, which was drawn at 20  $\text{min}^{-1}$  compared to that of the water-drawn film and monofilament, which were drawn at a strain rate of 2–3  $\text{min}^{-1}$ . Thus the axial residual stress will be the highest for the LOY-based sample and relatively lower for the film and monofilament. The cracks in LOY-based fiber are predominantly perpendicular to the fiber axis but form a tight spiral with a small pitch. This indicates that the transverse residual stress is much smaller than the axial residual stress. This results in a biaxial stress field whose resultant makes a small angle with the fiber axis. Helical cracking occurs as it generates the largest and most continuous surface area per unit volume in a cylindrical body and therefore represents the most efficient conversion of strain energy into crack surface energy.<sup>13</sup>

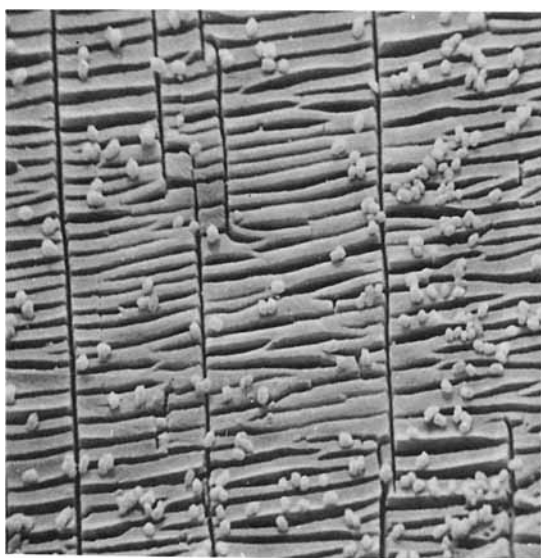
Compared to the LOY-based fiber, the axial residual stress in the monofilament and film is less because they have been produced at lower strain rate and low drawing stress. With lower axial residual stresses, the transverse cracks that form in these samples do not have to travel as far they do in the LOY-based fiber to relieve the stored energy. It is interesting to note that most of the transverse cracks that form in the thick monofilament and film never traverse more than a small part of the surface of the sample. Another noteworthy feature of the crack patterns in these samples is the presence of distinct longitudinal cracks, which suggests that the transverse stress is not insignificant in comparison to the axial stress.

### Heat-Set Samples

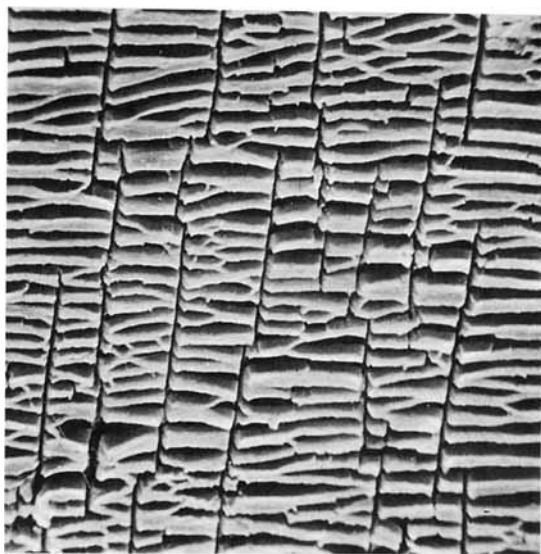
The crack patterns of as-drawn samples heat-set at various temperatures under the constant length and free-to-shrink conditions after etching in methylamine under identical conditions for 4 h will now be discussed. The structural characteristics of heat-set fibers are described elsewhere.<sup>11</sup>

The micrographs of the taut- and free-annealed film samples heat set at 100°C are shown in Figures 2(a) and (b). There are three noteworthy observations. First, the longitudinal cracks have now become more regular. Second, the transverse crack density has increased substantially. Third, the network nature of the crack patterns is retained. To explain these observations, it should be recalled that the

heat setting of the film sample at 100°C, viz. at a temperature above  $T_g$ , could be expected to even out the local residual stress distribution in the sample to a large extent. When the stress distribution is uneven, the cracks will form in regions that are highly stressed and due to this irregular cracks at a few places will form, as was the case in as-drawn sample. With more uniform residual stress distribution, the stress pattern will become more regular and the crack density could increase. In addition, the additional crystallization that occurs due to an-

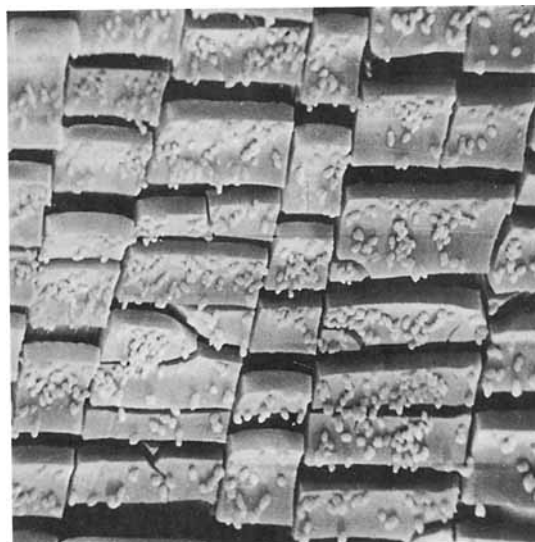


(A)

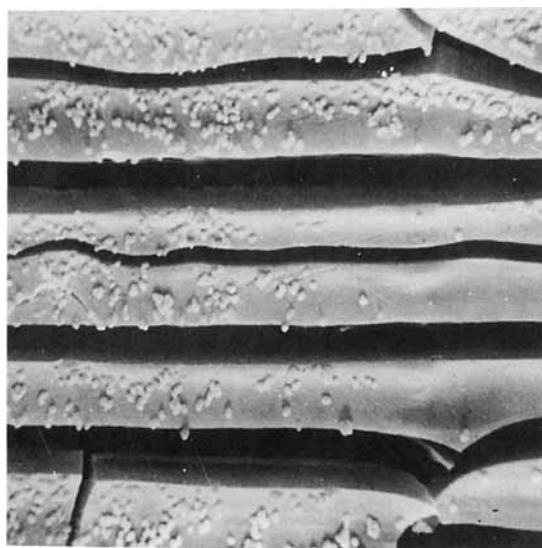


(B)

**Figure 2** Crack patterns in amine-etched heat-set PET film samples: (a) TA 100 ( $\times 770$ ) and (b) FA 100 ( $\times 717$ ).



(A)

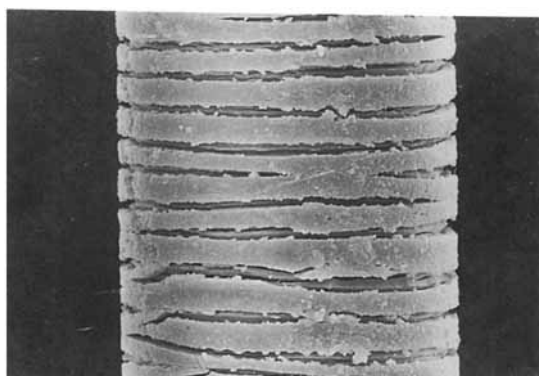


(B)

**Figure 3** Crack patterns in amine-etched heat-set PET film samples: (a) TA 220 ( $\times 752$ ) and (b) FA 220 ( $\times 752$ ).

nealing could also contribute to the stress field. This aspect is discussed later. However, since the crystalline and amorphous phases are not distinctly separated, the network structure will be retained. Similar observations were made in the case of the monofilament heat-set at 100°C and therefore the crack patterns in these samples are not reproduced here.

The micrographs of TA and FA samples of film heat-set at 220°C and TA and FA samples of monofilament heat-set at 200°C and TA sample of LOY-



(A)



(B)

**Figure 4** Crack patterns in amine-etched heat-set monofilament: (a) TA 200 ( $\times 680$ ) and (b) FA 200 ( $\times 680$ ).

based fiber heat-set at  $200^{\circ}\text{C}$  are shown in Figures 3(a) and (b), 4(a) and (b), and 5, respectively. The TA and FA samples of film show a remarkable difference in the crack pattern in that while only transverse cracks are observed in the FA sample, the TA sample shows longitudinal cracks also. The internal stresses in taut annealed samples will be expected to be relatively higher as they are constrained from shrinkage during heat setting, and therefore structural reorganization is impeded and distinct phase separation is not allowed to occur.<sup>11</sup> Though similar behavior is expected from monofilament also, both TA and FA samples show the same behavior. On close examination, the TA sample does show a slightly inclined helical geometry compared to the FA sample in which the spirals are flat. This suggests that the TA sample annealed at  $200^{\circ}\text{C}$  has relatively higher transverse stresses than the corresponding FA sample. At higher temperature of heat-setting ( $250^{\circ}\text{C}$ ), the stresses have relaxed to a large extent and the crack density is now low in both the cases [Figs. 6(a) and (b)].

An attempt will now be made to analyze the crack patterns in terms of sample morphology. The increase in crack density on annealing observed earlier may be due to the redevelopment of a new residual stress field due to crystallization, as observed by Sweet and Bell.<sup>1</sup> The origin of internal stress on crystallization has been explained as follows.<sup>14</sup> The crystallites are formed within the random entanglements of macromolecules. Since chain molecules are much longer than the crystallites, growth of linked crystalline regions must give rise to internal stress owing to the mutual hindrances. Thus, the faster the crystallization, the more stressed is the polymer, and farther its state from equilibrium. Kawai et al.<sup>15</sup> have proposed a model for crystallization process under molecular orientation according to which the link molecules between the crystals become more taut with crystallization, thus increasing the stress. It must also be remembered that additional stresses would be introduced as the sample is cooled after the heat treatment to room temperature. These will arise as a result of the difference in the coefficient of contraction between the crystalline and the amorphous phase.

As reported earlier,<sup>16</sup> the film and monofilament samples crystallize faster than the LOY-based yarn. The increase in crack density in the film annealed at  $100^{\circ}\text{C}$  can be attributed to this. However, at the highest temperature used, the stress can relax due to enhanced molecular mobility. The above model is adequate to explain the present result.

The absence of longitudinal cracks and the low density of transverse cracks in samples heat-set at higher temperatures can be explained as follows. In samples heat-set in the slack condition in the temperature range between  $220$  and  $250^{\circ}\text{C}$  and in the taut state at  $250^{\circ}\text{C}$ , the separation of the two phases has been shown<sup>17</sup> by low-angle X-ray diffraction to

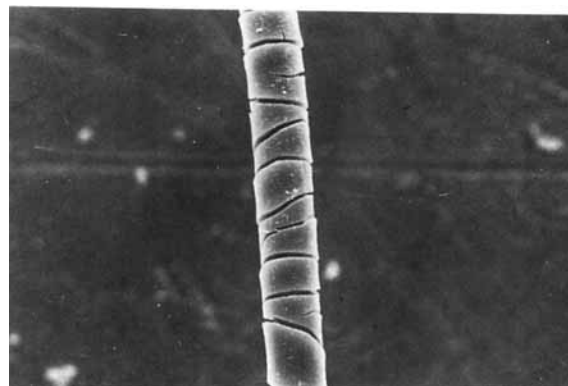
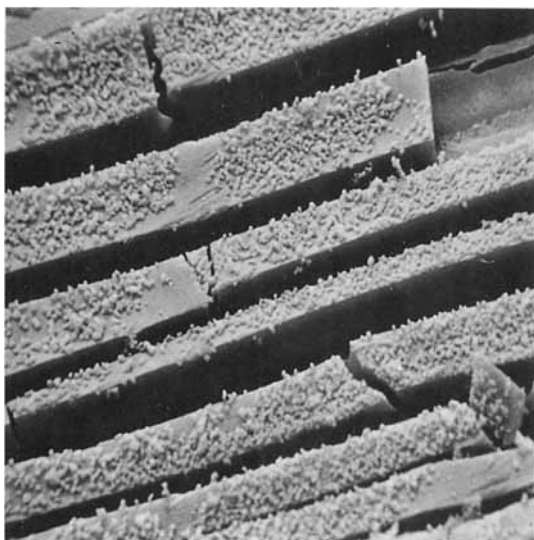
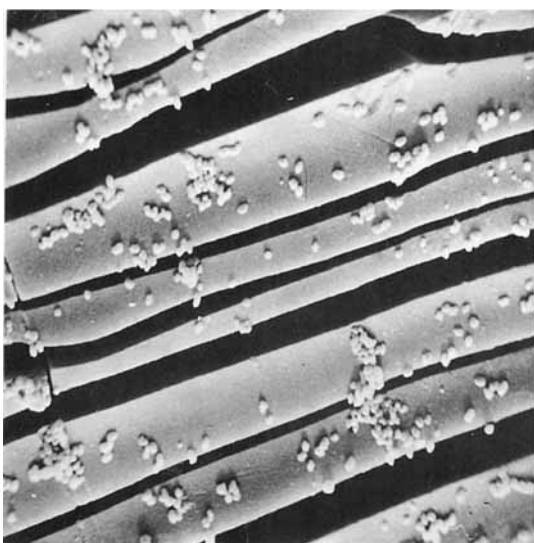


**Figure 5** Crack patterns in amine-etched LOY-based drawn fiber: TA 200 ( $\times 720$ ).



(A)



(B)

**Figure 6** Crack patterns in amine-etched heat-set PET film samples: (a) TA 250 ( $\times 770$ ) and (b) FA 250 ( $\times 735$ ).

be quite distinct. The amorphous regions in these samples have also very low amorphous orientation and are therefore fluidlike. This structural transformation apparently results in significant relaxation of the residual stresses. This is further discussed below.

On the basis of wide- and small-angle X-ray diffraction studies made on uniaxially drawn PET films that were not subsequently heat-set, Casey<sup>18</sup> proposed a fibrillar model for as-drawn PET film sample with 3-nm wide fibrils that were almost joined together. Such a joining together of crystallites in the

lateral direction has been proposed for cold-drawn isotactic polypropylene on annealing.<sup>19</sup> More recently thin polymer films from a solution of high-molecular-weight PET were spun at wind-up speed of 20 cm/s, and the proposed model for micellar morphology deduced from transmission electron microscopy for the as-spun and annealed (180°C) samples suggests the joining together of the micelles in the lateral direction.<sup>20</sup> As a result of the fusion of the crystallites in the lateral direction, the interfibrillar amorphous phase is likely to disappear and the transverse residual stress will relax. Consequently only the axial residual stress will remain and give rise to transverse cracks.

In the case of LOY-based yarn (TA 200) there was a very significant reduction of crack density as compared to that of the control sample, indicating reduction of the residual stress.

## CONCLUSIONS

Chemical etching of the PET samples by 40% aqueous methylamine introduces stress crack patterns on the film and fiber surfaces. These patterns have been examined on a scanning electron microscope, and it has been shown that they are significantly affected by the process variables. On heat setting, the samples showed significant differences in their crack patterns. An attempt has been made to correlate the etch patterns to sample morphology.

The authors wish to thank Mr. D. C. Sharma of the SEM Laboratory, Indian Institute of Technology, New Delhi, India, for the SEM micrographs.

## REFERENCES

1. G. E. Sweet and J. P. Bell, *J. Polym. Sci., Polym. Phys. Ed.*, **16**, 2057 (1978).
2. G. E. Sweet and J. P. Bell, *J. Polym. Sci., Polym. Phys. Ed.*, **16**, 1935 (1978).
3. R. Murray, M. A. Davis, and P. Tucker, *J. Appl. Polym. Sci., Polym. Symp.*, **33**, 177 (1978).
4. R. S. Chauhan, M. V. S. Rao, and N. E. Dweltz, *J. Appl. Polym. Sci.*, **30**, 19 (1985).
5. W. P. Baker, *J. Polym. Sci.*, **57**, 993 (1962).
6. C. M. Chu and G. L. Wilkes, *J. Macromol. Sci., Rev. Macromol. Phys. Chem.*, **B10**, 551 (1974).
7. G. C. Adams, *Polym. Eng. Sci.*, **16**, 222 (1976).
8. D. T. Duong and J. P. Bell, *J. Polym. Sci., Polym. Phys. Ed.*, **13**, 765 (1975).
9. R. E. Mehta and J. P. Bell, *J. Polym. Sci., A-2*, **11**, 1793 (1973).
10. D. C. Prevorsek, R. H. Butler, V. D. Kwon, G. E. R.

- Lamb, and R. K. Sharma, *Text. Res. J.*, **47**, 107 (1977).
11. V. B. Gupta and S. Kumar, *J. Appl. Polym. Sci.*, **26**, 1865 (1981).
  12. Ch. Oudet and A. R. Bunsell, *J. Mat. Sci.*, **22**, 4292 (1987).
  13. J. K. Gillham, P. N. Reitz, and M. J. Doyle, *Polym. Eng. Sci.*, **8**, 227 (1968).
  14. A. Strepikhevev, V. Derevitskaya, and G. Solninsky, *A First Course on Polymer Chemistry*, MIR Publishers, Moscow, 1971, p. 127.
  15. T. Kawai, M. Iguchi, and T. Tonami, *Kolloid-Z-u. Z. Polym.* **221**, 28 (1968).
  16. V. B. Gupta, J. Radhakrishnan, and S. K. Sett, *Polymer*, **34**, 3814 (1993).
  17. V. B. Gupta, C. Ramesh, and A. K. Gupta, *J. Appl. Polym. Sci.*, **29**, 3115 (1984).
  18. M. Casey, *Polymer*, **18**, 1219 (1977).
  19. A. Ferraro, E. Ferracini, and R. Hosemann, *Polymer*, **25**, 1747 (1984).
  20. J. Petermann and U. Reick, *J. Polym. Sci., Polym. Phys. Ed.*, **25**, 279 (1987).

Received June 6, 1994

Accepted July 19, 1994